Study Of The Effects Of Channel Design On The Performance Of The Polymer Electrode Membrane Fuel Cell

Yasir Abduwahhab Abed Al-Okbi
Lecture Assistant
University of Baghdad
yasir.alokbi@gmail.com

Abstract:-

This work is concerned with some key aspects relating to design of an integrated proton exchange membrane fuel cell and metal hydrides storage vessel provide efficient hydrogen storage for different applications, containing low temperature polymer electrode membrane (PEM) fuel cells. The metal hydrides systems use unsteady hydride supplies (equilibrium H_2 pressure at ambient temperature around 10 bar) both liquid and air heated cooled, and optimized system layout, facilitates H_2 supply to low temperature polymer electrode membrane fuel cell stacks. Study and analysis of all currently used storage methods was undertaken, and performance of the fuel cell. A full design task was undertaken with specific attention given to fluid flow regulation and heat transfer in the fuel cell. Computational fluid dynamics (CFD) were completed to fully inform design decisions a confirm success. An electrical system was also designed to compute control of the components. All items were manufactured and the fully functioning system was tested.
This research concludes the fuel cell voltage was outstanding although reduced time for testing resulted in it dropping short with respect to power and current. It was found that the rectangular channels produced a 0.3W. Furthermore, the stack combined heat and power efficiency was determined to be 52 % and the integrated system total efficiency was 40 %. Finally the cost analysis showed that the payback period of the capital cost invested on the integrated system during a few years.

Keywords: polymer electrode membrane, fuel cells, heat transfer, storage vessel, control volume-based finite difference scheme.

1. Introduction

A hydrogen storage vessel is simple in principle; it utilizes an intermetallic compound in the form of a powder to absorb hydrogen into its structure which can then be released when needed by the application of heat [9]. This compound is often referred to as a metal hydride. During the absorption cycle is added hydrogen to the compound, the capacity and rate of uptake are dependent on temperature and pressure conditions as well as the

absorbing material. This process is exothermic causing heat to be released and increasing the temperature of the powder [10]. During desorption, the process of removing hydrogen from the compound, the rate of release is dependent on the temperature and pressure. This is an endothermic process, resulting in a drop of temperature [2]. In order to be practically useful the temperature and pressure are controlled during absorption and desorption to achieve the desired characteristics. A specially designed pressure vessel is often used in order to store the powder, which in addition to withstanding pressure, must also allow for heat transfer. Fuel cell operation is slightly. More difficult to explain the principles of operation are best explained by the following steps:

1. Two hydrogen atoms are split at an anode catalyst into their proton and electron parts.

2. The adjacent proton exchange membrane allows only the protons to pass though.

3. The electrons are conducted away through the anode around an electrical circuit.

4. At the cathode, four protons, four electrons, and one diatomic oxygen then react to provide water. This is also an exothermic process so the water is warm.

In order for this reaction to take place, a surrounding structure and assisting components are needed. To improve distribution of gas across the catalyst anode and cathode a flow field plate is utilized. This is a conductive plate which allows for gas flow and makes up the bulk of solid material in the stack. This can be seen in **Fig. 1**. The next improving component is the gas diffusion layer.

Fig. 1 Diagram to explain fuel cell basic operation. [2]

This is between the catalyst and flow field plate and aids gas diffusion across the catalyst and moisture control [11]. The separate parts of the reaction area are also isolated though the use of sealants, and cooled using fluid flow through the stack.

2. Mathematical Model

The governing equations. corresponding to the various regions of the fuel cell are given below. The flow in the reactant gas channels is governed by the Navier–Stokes equation [13, 6].

Continuity Eq.

$$\frac{d\rho}{dt} + \nabla \times (\rho \times u) = 0 \qquad (1)$$

Momentum Eq.

$$\rho \times \frac{du}{dt} + \rho(u \times \nabla)u = \nabla \times [-pI + \tau] + F \quad (2)$$

Energy Eq.

$$\rho\left(\frac{dU}{dt} + u \times \nabla U\right) - \nabla \times (K_H \nabla T) + p\nabla \times u) = 0 \quad (3)$$

These form the continuity equation (1) which is used to represent the conservation of mass, the conservation of momentum (2) and the conservation of energy (3). Where:

* ρ is the density ($k.gm^{-3}$)
* u is the velocity vector ($m.s^{-1}$)
* p is the pressure (Pa)
* I is the index matrices
* μ is the dynamic viscosity ($Pa.s$)
* F is the force vector ($N.m^{-3}$)
* KH is the heat conduction coefficient ($W.m^{-2}K^{-1}$)
* T is the absolute temperature (K)
* ∇ is the Del operator
* τ is the viscous stress tensor (Pa) given by:

$$\tau = 2\mu S - \frac{2}{3}(\nabla \times u) I \quad (4)$$

* And S is the strain-rate tensor given by the Eq.

$$S = \frac{1}{2}(\nabla u + (\nabla u)^T \quad (5)$$

The strain and stress tensor are used to solve the Navier-Stokes equations to output the required results [4, 5].

3. Test Procedure

The evaluation of the fuel cell design requires that single pairs of each design of plate be tested under various operational conditions and performance curves are shown. In order to establish the operating performance of the fuel cell, the system was manipulated by changing the flow of hydrogen and air. A power resistor was used to load the fuel cell over time at a specific resistance and to ensure that the fuel cell was operating. This is seen in **Fig. 2**.

The check valves CV2 and 3 are used to control and maintain the pressure within the fuel cell,

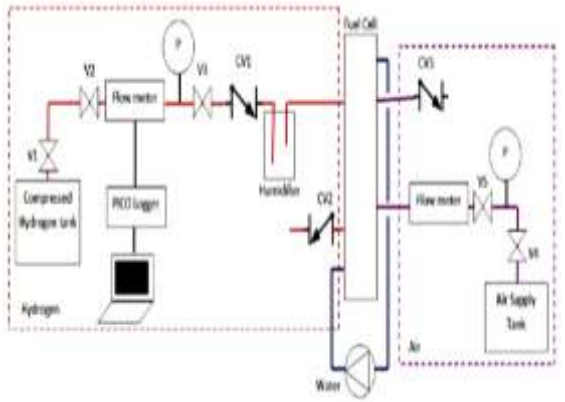

Fig. 2 Fuel Cell Test Setup

By setting them to maintain 1 bar internal pressure. The pico logger records the flow of hydrogen from the storage tank into the fuel cell. Valves V2 and V4 are used to modify the flow of the gases into the fuel cell. This can be seen in **Fig. 3**.

Fig. 3 Fully assembled single stack Fuel Cell

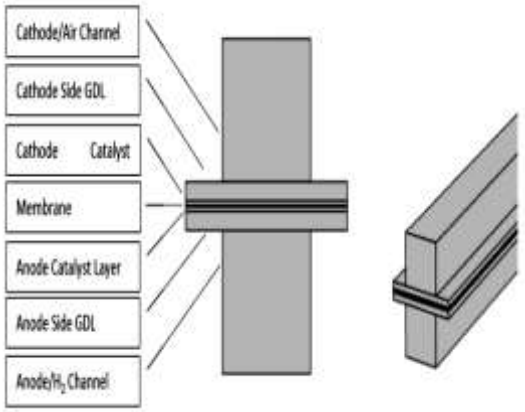

Fig. 4 Simplified geometry used in Ansys. It represents an anode and cathode side channel, the GDLs, the catalytic layers and the proton exchange membrane

4. Boundary Conditions and Parameters

The boundary conditions set depend on analysis of the plate is analyzed in two dimensions to find the velocity and pressure. The same assumptions are also applied (the flow is modelled as laminar, the hydrogen is an ideal gas, temperature across the plate is uniform and there is a no slip wall boundary condition). The results were then used to calculate the mass transfer coefficient across the plate, using the equations shown above. The parameters used in the modelling can be seen below.

This study was done on a small section of the fuel cell to represent and model the potential behavior of the system as accurately as possible without causing over complication due to the high complexity of the multiphase model. This complexity due to design the channel of fuel cell for each hydrogen and oxygen plates. The simplified geometry can be seen in **Fig. 4.**

The size of the geometry is modelled from the square channel flow field plates. The triangular channels would have been modelled as well but due to time constraints and the difficulties in learning the program this could not be achieved. This analysis simulates the diffusion and mass transfer of hydrogen and oxygen into the GDL and catalytic layers using the Maxwell-Stefan diffusion model as well as the Navier-Stokes equations to obtain momentum transfer. The electrochemical reaction is modelled with the Butler-Volmer equation. In the anode side channel, hydrated hydrogen is present and in the cathode channel, air is modelled flowing through it. The air is modelled as nitrogen, oxygen and water vapour. The model is solved for a range of voltages from 0.9V to 0.15V. The model outputs a polarisation plot for the cell and the concentrations of hydrogen, oxygen and water in their respective channels

and GDLs. The model assumes that the flow of gases is laminar, there is a no slip boundary condition on the walls, every boundary apart from the anode and cathode rib lengths is electrically isolating and no water is involved in proton transfer [9]. The velocity at the inlets was taken from the flow field analysis of each plate. The list of parameters used in the model can be seen in **Table1**.

Table. 1 Model Parameters

Name	Expression	Description
W_rib	1.5e^-3(m)	Rib width
H_gdl	0.2(mm)	GDL width
H_electrode	50e^-6(m)	Porous electrode thickness
H_membrane	0.01(mm)	Membrane thickness
eps_gdl	0.4	GDL porosity
Kappa_gdl	1.76e-11(m^2)	GDL permeability
Sigma_gdl	222(s/m)	GDL Electric conductivity
WH2_in	0.9	Inlet H2 mass fraction(anode)
WH2O_in	0.023	Inlet H2O mass fraction (cathode)
WO2_in	0.228	Inlet oxygen mass fraction(cathode)
U_in_anode	0.212	Anode flow velocity
U_in_cathode	0.173	Cathode flow velocity
Mu_anode	1.19e-5(pa.s)	Anode viscosity
Mu_cathode	1.19e-5(pa.s)	cathode viscosity
MH2	0.002(kg/mol)	Hydrogen molar mass
MN2	0.028(kg/mol)	Nitrogen molar mass
MH2O	0.018(kg/mol)	Water molar mass
MO2	0.032(kg/mol)	Oxygen molar mass
D_H2_H2O	9.15e-5.(?/307.1(k))^1.75(m^2/s)	H2_H2O binary diffusion coefficient
D_N2_H2O	2.56e-5.(?/307.15(k))^1.75(m^2/s)	N2_H2O binary diffusion coefficient
D_O2_N2	2.2e-5.(?/293.2(k))^1.75(m^2/s)	O2_N2 binary diffusion coefficient
D_O2_H2O	2.82e-5.(?/308.1(k))^1.75(m^2/s)	O2_H2O binary diffusion coefficient
T	70+273.15(k)	Cell temperature
P_ref	101e3(pa)	Reference pressure
V_cell	0.9	Cell voltage
O2_ref	40.88(mol/m^3)	Oxygen reference concentration
H2_ref	40.88(mol/m^3)	Hydrogen reference concentration
eps_l	0.3	
eps_l	1-eps_1-eps_gdl	Open volume fraction for gas diffusion in porous electrodes
Kappa_l	Kappa_gdl/s	Permeability(porous electrode)
Sigma_m	9.825(s/m)	Membrane conductivity

5. Flow Field Analysis

A bipolar plate has dozens of fine channels to distribute the reactant and oxidant over the fuel cell. The size, shape and pattern of the flow channel significantly affect the performance of PEMFC. Water management is one of the major issues in PEMFC so if the flow channel is poorly designed, certain regions in the flow channels will remain flooded with water (product of PEMFC, mostly in cathode side) and block the incoming gas, thereby depleting the performance of a fuel cell. Such blocked regions not only reduce the performance of PEMFC but also can cause irreversible damage to the fuel cell (i.e. corrosion and material degradation of the plate). As far as the flow field design is concerned, the serpentine flow is the best option. Serpentine flow offers high pressure drop due to long channels which ensures uniform distribution of reactants. Also the water droplet which blocks the flow channels is removed due to the high pressure difference which forces the water out of the channels. Although the elimination of condense water in the cathode is improved, the energy required to drive the gas increases (like a blower), reducing the overall performance of the PEMFC. In serpentine type flow fields, longer straight channel segments (narrower channels) between channel bends also enhance convection. To reduce the pressure drop, multi-serpentine channels are used to offer considerable pressure drop while maintaining good water management [1,3].

6. Results and Discussion

The results from the electrochemical analysis show the theoretical polarisation plot for the fuel cell **Fig.**

5. The model gives a maximum current density for 0.15V at 0.769A/cm^2. The results indicate that the maximum power output from the cell would occur at 0.45V, giving 6.3W.

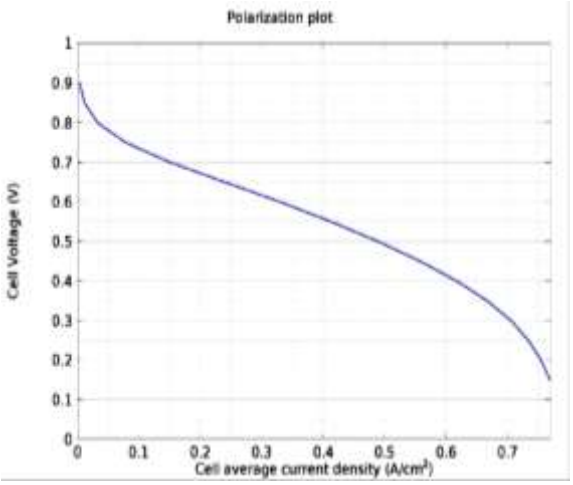

Fig. 5 Theoretical polarisation plot the fuel cells performance.

The results also show where the current would be formed during the cells operation. At 0.8V **Fig. 6** it can be seen that the largest current is produced close to the inlet of the channel but not directly above the channel, above the walls of the channel and in the rib between channels. Above the channel there can be seen to be very little current produced. This could be a by-product of the geometry and could change with triangular channels in the future work. In contrast to the concentration of hydrogen, the current appears highest where there is the least amount of hydrogen **Fig. 7**. In fact it is where the highest concentration of water vapor occurs in the GDL and catalytic layer. At this voltage, there is a dramatic difference in concentration between anode and cathode water concentration.

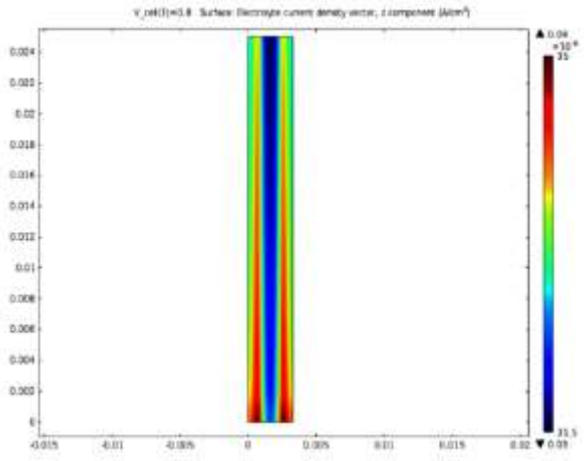

Fig. 6 A map of the current density at 0.8V.

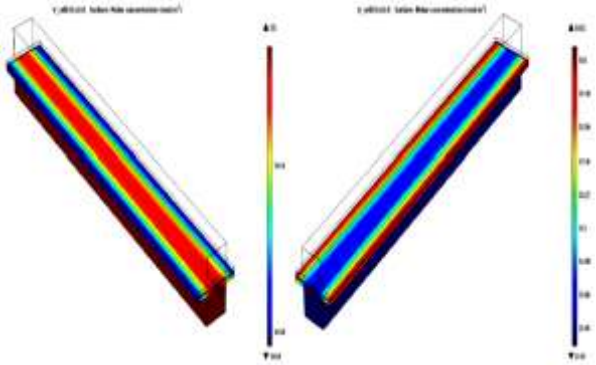

Fig. 7 Concentration of hydrogen (left) and water vapour (right) in the anode side of the cell in mol/m^3 at 0.8V.

At the anode side, there is a maximum water concentration of 0.61mol/m3 however at the cathode side there is a maximum of 1.47mol/m^3 (Fig. 8). This is due to the reaction in the fuel cell. **Fig. 14** also shows the disapation of the water through the channel, there is a concentration difference between the inlet and outlet of 0.05mol/m^3. At the

cells maximum power, 0.45V, there is a substatial difference in the behavior of the cell. The current density **Fig. 9** is closer to the initial ideas of what would happen in the cell.

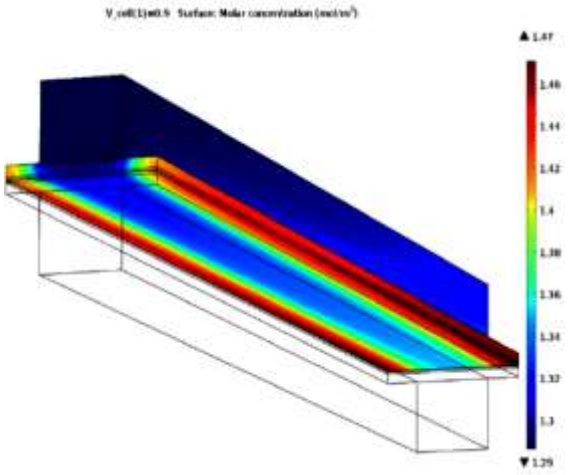

Fig. 8 Water concentration in mol/m3 in the cathode side of the cell

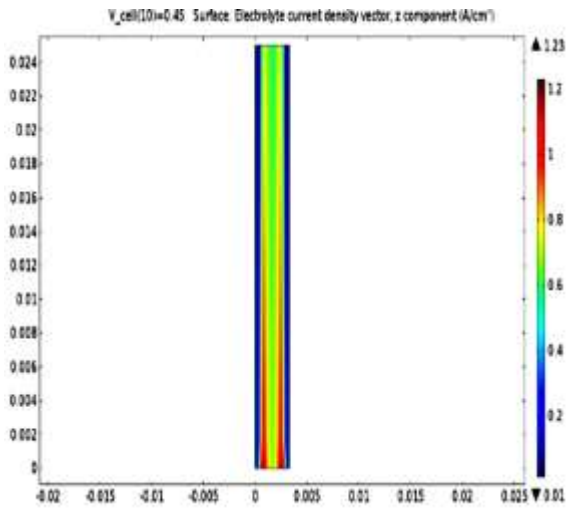

Fig. 9 A map of current density produced at a voltage of 0.45V.

Most noticeably, there is a greater current density being produced above the channel compared to 0.8V. At the center of the channel, there is a difference of 0.1A/cm^2 being produced from inlet to outlet. It is now greater than that produced at the rib however the greatest current density can still be seen above the walls of the channel towards the inlet. Comparing again the distribution of hydrogen and water to the current density is shown in Fig. 10. With a higher load on the cell, the hydrogen has diffused into the membrane to a much greater extent. Interestingly, there is a considerable lack of hydrogen by the inlet GDL compared to the outlet, a difference of 4.63mol/m^3. This is because of the high water concentration by the inlet, a value of 8.43mol/m^3. As the load has increased the reaction rate has increased with it **Fig. 11** and so the production of water is higher. Compared to 0.8V the maximum has greatly increased to 15.1mol/m3 and is saturating most of the membrane area. The concentration of oxygen also reveals that the water is being dragged to the outlet with the air. Similar to the larger voltage, it appears that most of the water is created at the fringes of the membrane although at 0.45V there is now a substantial creation of water above the channel towards the outlet. Finally looking at the highest current density calculated by the model, 0.15V, the behavior and results of the cell are similar but exaggerated. The surface plot of current density **Fig. 12** shows a similar trend to that of the difference between 0.8 and 0.45V, the highest current density is found just above the walls of the channel at the inlet. The value here is quite high,

2.55A/cm^2, however due to the lower current density across the rest of the face the average is brought down to 0.769A/cm^2. The concentration of hydrogen in the membrane has further increased as the load across the cell increases **Fig.13**, especially towards the outlet of the cell where the concentration reaches 32.7mol/m^3. The water concentration is still highest by the inlet, at a value of 9.35mol/m^3, only slightly higher than at 0.45V. Clearly the highest current density occurs at where the membrane is most hydrated. The cathode side of the cell shows that at this high current density nearly the entire membrane is full of water at an average concentration of 14.2mol/m^3 **Fig. 14**.

The reaction is producing a lot of water at this point and could be limiting the reaction rate. Looking at the underside of the cathode, there is very little variation in water concentration meaning that the cell may not be able to get rid of the level of water created effectively. Further modelling would need to be done to see how the level of water creation at various reaction rates affects the state of the cell.

The flow of air, 130 cc/min and hydrogen, 123.49 cc/min, was set and an IV curve was generated from the sourcemeter, shown in **Fig. 15**. The peak power, for the quadrilateral channel design is around 0.65Watts. This is lower than predicted, but shows that the fuel cell is operating correctly. Further investigation of air and hydrogen flows, and their respective voltage and power curves, is required to fully investigate the potential of the fuel cell.

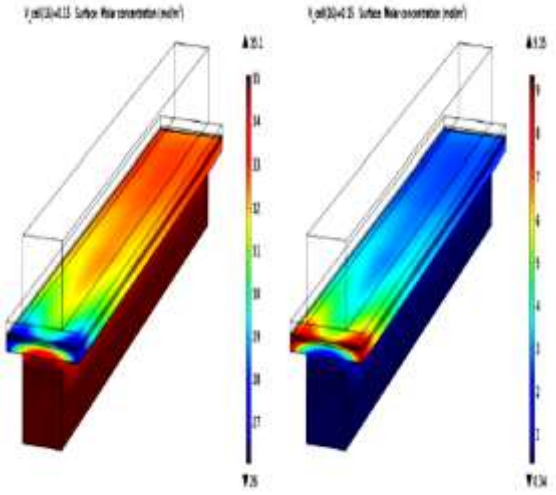

Fig. 10 Hydrogen concentration (left) and water concentration (right) in mol/m^3 at 0.45V in the anode side of the

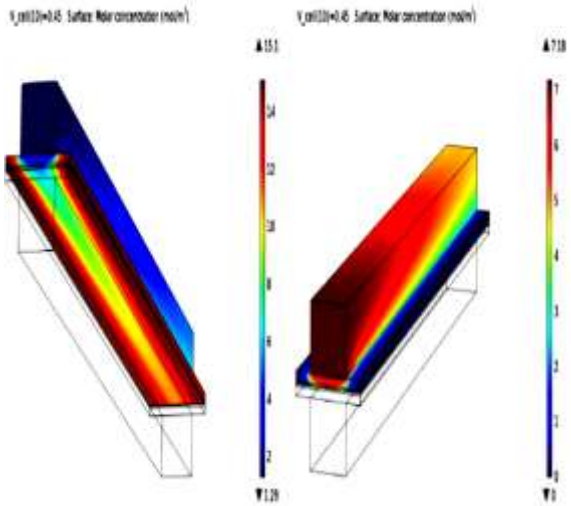

Fig. 11 Water (left) and oxygen (right) concentration in the cathode side. Measured in mol/m^3

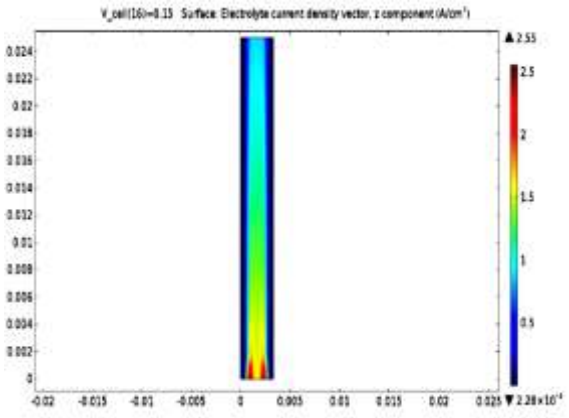

Fig. 12 Surface map of the

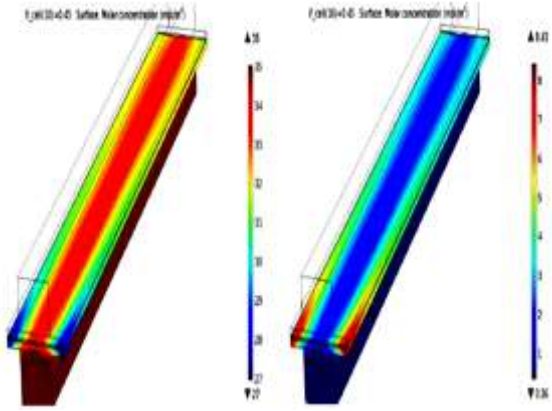

Fig. 13 The concentrations of water (left) and oxygen (right) in mol/m^3

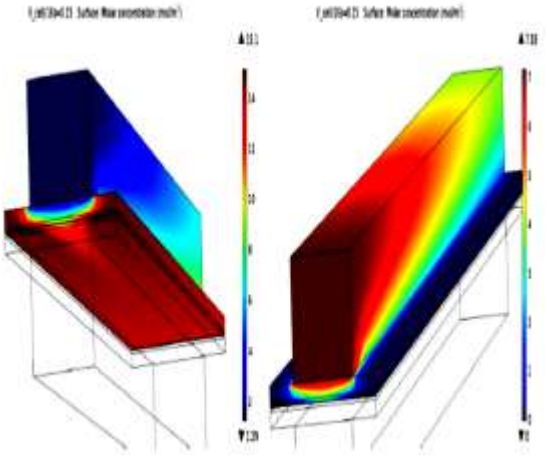

Fig. 14 The concentrations of water (left) and oxygen (right) in mol/m^3.

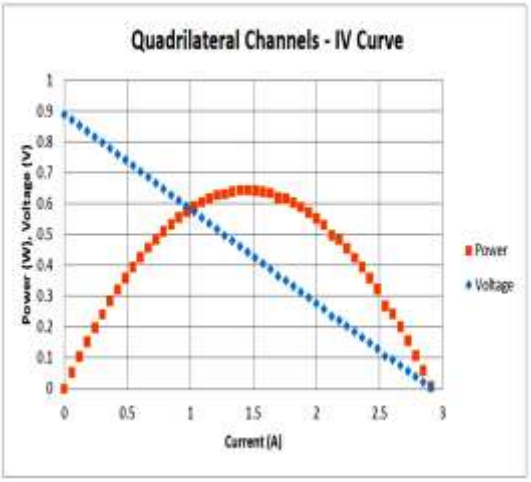

Fig. 15 IV-Curve for single stack of channel plates

7. Conclusions

The aim of the project is to design and manufacture an integrated metal hydride storage vessel and combined heat and power proton exchange membrane fuel cell with an electrical control system. The purpose of the project is to use new or innovative techniques to improve on fuel cell performance.

A fuel cell will be designed in order to convert the hydrogen released from the storage vessel into as much usable energy as possible. Although many fuel cell types are available a PEM Fuel Cell will be utilized. The design of the fuel cell represents further design challenges such as routing hydrogen, air, and water, to alternating sides of the flow field plates though carefully managed flow channels and back out of the cell whilst also remaining completely sealed. The design of these channels are to be optimized for minimum

drop in pressure, optimum velocity, pressure balance from one side of the membrane to the other, and an even distribution in pressure across each channel. In addition to the complexity already shown, temperature measurements must be taken as close as possible to the reaction site in the centre of the cell for optimal control over the rate of reaction and electrical production efficiency. The designed system will provide 91% of the annual electrical load and 50% of the annual heating load. For this, a PEMFC was designed with optimised flow channel configuration for bipolar plates. The IV curve of the designed PEMFC was used to design the fuel cell subsystem and heating data from literature was used to make a combined heat and power system system. The system used for fuel processing for the PEMFC stacks was biomass gasification. The fuel cell processing system was designed with reference from the literature and its operating conditions were set accordingly. Then the fuel cell and fuel processing system was couple into an integrated combined heat and power system

Key Findings:

- Existing PEMFC showed low efficiency due to ohmic losse resulting from low conductivity and low potential of the Memebrane Electrode Assembly to uptake water to keep itself hydrated.
- Wide channels of the existing PEMFC also lowered the efficiency due to low reactant convection and diffusion to the gas diffusion layer.
- Oxygen was fully depleted from the quadruple squared flow channel before oxygen reached the end of the newly bipolar plate design which was also confirmed by Lui et. al for their quadruple flow channels.
- The total heat and electrical efficiency of the stack system was 52 % which is lower than the usual 80% combined heat and power system efficiency but it was in the range of 47-60 % PEMFC stack combined heat and power system efficiency of Chutichai et.al.
- Cost of a large capacity combined heat and power system fuel cell system (like 25-100 KW) have low cost compared to small capacity system (1-5 KW) and small variations in cost of fuel cell combined heat and power system system with the annual manufacturing rate.

References

[1] A.P. Manso , F.F. Marzo , J. Barranco , X. Garikano , M. Garmendia Mujika . (2012). Influence of geometric parameters of the flow fields on the performance of a PEM fuel cell. A review. International journal of hydrogen energy. 37 (20), p15256-15287.

[2] B. Charlas, A. Chaise, O. Gillia, P. Doremus and D. Imbault, “Investigation of hydride bed

swelling and shrinking during hydrogen absorption/desorption cycles under different compressive stresses," Journal of Alloys and Compounds, vol. 580, pp. S149-S152, 2013.

[3] Chutichai, B., Authayanun, S., Assabumrungrat, S., Arpornwichanop, A. (2013)'Performance Analysis of an Integrated Biomass Gasification and PEMFC (Proton Exchange Membrane Fuel Cell) System: Hydrogen And Power Generation', Energy, 55(1), pp. 98-106.

[4] Clay Mathematics Institute. "Navier-Stokes Equations." http://www.claymath.org/Millennium_Prize_Problems/NavierStokes_Equations/.

[5] Faber, T. E. Fluid Dynamics for Physicists. New York: Cambridge University Press, 1995. and comparison of various designs of gas http://www.frontiersin.org/Journal/Abstract.aspx?s=1462&name=fuel%20cells&ART_DOI=10.3389/fenrg.2014.00002 flow fields to PEM fuel cells and cell stack performance.

[6] Hu M, Gu A, Wang M, Zhu X, Yu L. Three dimensional, two phase flow mathematical model for PEM fuel cell: part I. Model development. Energy Convers Manage 2004; 45:1861–82.

[7] Liu H, Li P, Juarez-robles D, Wang K and Hernandez-guerrero A .(2014) Experimental study

[8] M. Alexandre, "Introduction of an integrated photovoltaic-regenerative fuel cell power system for an average London house," London, 2014.

[9] M. V. Lototskyy, M. W. Davids, I. Tolj, Y. V. Klochko, B. S. Sekhar, S. Chidziva, F. Smith, D. Swanepoel and B. G. Pollet, "Metal hydride systems for hydrogen storage and supply for stationary and automotive low temperature PEM fuel cell power modules," International Journal of Hydrogen Energy, vol. 30, pp. 1-7, 2015.

[10] Proton Motor Fuel Cell, Basic Operation of a Fuel Cell, Puchheim: Proton Motor Fuel Cell, 2012.

[11] T. Cargnel and Z. Dehouche, "Deisgn of a hydrogen storage cylinder," 2014.

[12] V. Mehta and J. S. Cooper, "Review and analysis of PEM fuel cell design and manufacturing," Journal of Power Sources, vol. 114, pp. 32-53, 2002.

دراسة تأثيرات تصميم القناة على كفاءة القطب الكهربائي ذو الغشاء البوليمرية المستخدم في خلايا الوقود

ياسر عبد الوهاب عبد

مدرس مساعد

جامعة بغداد

الخلاصة:-

هذا العمل يتناول بعض الجوانب الرئيسية المتعلقة بتصميم خلية وقود متكاملة ذات غشاء تبادل البروتون مع وعاء خزن مكون من مركب ثنائي من المعدن والهيدروجين (metal hydrides) ليزيد من كفأة الهيدروجين لخزن الطاقة في مختلف التطبيقات، والتي تتضمن خلايا الوقود ذات الغشاء البوليمري ذات درجة حرارة منخفضة أنظمة المركب الثنائي من المعدن والهيدروجين (metal hydrides) تستخدم مصادر هيدريد غير مستقرة) حيث يتم توازن ضغط H2التوازن عند درجة الحرارة المحيطة حوالي 10 بار (كلا من المائع والهواء يكون ساخن بارد و التصميم الامثل للمنظومة يوفر مصدر هيدروجين لخلية الوقود ذات الغشاء البوليميري المنخفضة الحرارة . الدراسة و التحاليل الحالية تركز على طريقة التخزين ، وأداء خلية الوقود. التصميم الامثل يركز على تنظيم تدفق السوائل وانتقال الحرارة في خلية الوقود. فقد تم استخدام ديناميكة الموائع (CFD) لحل المعادلات وايجاد التصميم الامثل لخلية الوقود لضمان عملها بنجاح. اما النظام الكهربائي فقد تم تصميمه لغرض السيطرة على المكونات الخلية. جميع المواد والمكونات اللازمة تم تصنيعها واختبار النظام والتاكد من انه يعمل بشكل جيد. وخلاصة ههذا البحث هو الحفض على فولطتية الخلية على الرغم من النقصان الحاصل في الزمن خلال الاختبار نسبة الى مقدار الطاقة والتيار. وقد تبين أن الخلية ذات القنوات المربعة أنتجت 0.3 واط. علاوة على ذلك تم تحديد الكفاءة الطاقة والحرارة مجتمعة لتصبح 52% وبلغت الكفاءة الكلية للنظام المتكامل 40٪. وأخيرا، أظهر تحاليل أن فترة استرداد التكاليف الرأسمالية المستثمرة على النظام المتكامل كانت قرابة بضع سنوات.

الكلمات المفتاحية:- القطب الكهربائي ذو غشاء البوليمر ،خلايا الوقود، فيض حراري منتظم ،ثبوت الحجم، طريقة الفروقات الحجمية.